Substituents Effects in POP Pincer Complexes of Ruthenium

Quinn Major,[†] Alan J. Lough,[‡] and Dmitry G. Gusev*,[†]

Department of Chemistry, Wilfrid Laurier University, Waterloo, Ontario, Canada N2L 3C5, and Department of Chemistry, University of Toronto, Toronto, Ontario, Canada M5S 3H6

Received January 25, 2005

Reactions of $[RuCl_2(p\text{-cymene})]_2$ with $(^tBu_2PCH_2CH_2)_2O$ (POP-^{t}Bu) and $(^iPr_2PCH_2CH_2)_2O$ (POP-^{i}Pr) afforded $RuCl_2$(POP-^{t}Bu) (**1**) and $[Ru_2(\mu\text{-Cl})_3$(POP-^{i}Pr$)_2]$Cl (**2**·Cl), respectively. The POP ligand is coordinated in a *mer* fashion in complex **1**, whose crystal structure revealed a γ-agostic C−H···Ru interaction of one ^{t}Bu group. Spectroscopic evidence indicated that this agostic interaction is retained in **1** in solution. A related compound, $[Ru(N_2)Cl$(POP-^{t}Bu)$]BPh_4$ (**4**), which also showed agostic bonding of a ^{t}Bu group, was obtained by substitution of N_2 for Cl^- in **1**, in the presence of $NaBPh_4$. Compound **2**·Cl readily underwent ion exchange with $LiBPh_4$ or $LiPF_6$ to give **2**·BPh_4 or **2**·PF_6 salts, respectively. A crystallographic analysis of **2**·PF_6 established a co-facial bioctahedral geometry of the $[Ru_2(\mu\text{-Cl})_3$(POP-^{i}Pr$)_2]^+$ cation containing two POP ligands coordinated in a *fac* fashion. Reactions of **1** and **2** with H_2 afforded the dihydrogen complexes *cis*,*trans*-$Ru(H_2)Cl_2$(POP-^{t}Bu) (**3**) and *cis*,*cis*-$Ru(H_2)Cl_2$(POP-^{i}Pr) (**5**), respectively. The H−H bond distances are very similar in both compounds, r(H−H) = 1.0 ± 0.1 Å, based on the T_{1min} and J_{HD} data and results of DFT calculations. Reaction of **2** with N_2 gave the dinitrogen complex *cis*,*cis*-$Ru(N_2)Cl_2$(POP-^{i}Pr) (**6**), but solutions of **1** under a nitrogen atmosphere showed no evidence of an analogous compound. The different steric requirements of the phosphorus substituents of the POP ligands were identified as the source of the differences in the coordination properties of the POP-^{t}Bu and POP-^{i}Pr complexes **1**−**6**.

Introduction

The importance of pincer ligands and their metal complexes to organic synthesis and catalysis has been recently underlined by the publication of two reviews.[1] Chart 1 renders a generalized structural drawing of a pincer complex featuring the characteristic *mer*-DGD tridentate ligand set. The reactivity of such systems is substantially altered by ligand modification, particularly by variations in the pincer ligand backbone, donor atoms, and their substituents. The donor atoms have a strong effect on the electron density at the metal center, whereas their substituents may create moderate to strong steric congestion around the metal to control its accessibility. Thus, fine-tuning of the reactivity of the pincer complexes for catalysis and organic synthesis can be accomplished through systematic manipulations of the DGD set.

An interesting type of pincer ligand is one incorporating an oxygen and two phosphorus donor centers in a POP fashion. In combination with a late transition metal this would result in formation of a M(POP) fragment with a weak O→M bond. This feature can enhance bonding of other groups to the metal center at the coordination site *trans* to the oxygen atom. The simplest POP pincer ligand geometry comprises a di-

Chart 1

M = metal
D and G = donor atoms
L = ancilary ligands

Chart 2

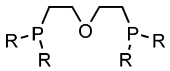

POP-R

ethyl ether backbone connecting two dialkyl or diaryl phosphine units (POP-R) as shown in Chart 2. A number of phosphorus substituents have been incorporated in this ligand including R = Ph, ^{t}Bu, Et, Cy, and the more exotic 3-pyridyl and 4-((diethylamino)methyl)-phenyl groups. However, only a small number of POP-based pincer complexes have been reported,[2] and only two, $ReCl_2(\equiv N)$(POP-Ph) and $[Rh(CO)$(POP-Ph)$]^+$,[2a,i] have been structurally characterized and their chemistry is underdeveloped. In the present work, our main objective was to obtain first POP pincer complexes of ruthenium and to study the effect of phosphine substitution on the reactivity and structure of such species. To this end, we used the known bis(2-(di-*tert*-butylphosphino)ethyl) ether ligand (POP-^{t}Bu) and prepared a new bis(2-(diisopropylphosphino)ethyl) ether ligand (POP-^{i}Pr) and isolated their ruthenium complexes from reac-

* To whom correspondence should be addressed. E-mail: dgoussev@wlu.ca.
† Wilfrid Laurier University.
‡ University of Toronto.

(1) (a) Singleton, J. T. *Tetrahedron* **2003**, *59*, 1837. (b) van der Boom, M. E.; Milstein, D. *Chem. Rev.* **2003**, *103*, 1759.

10.1021/om050053v CCC: $30.25
Publication on Web 04/12/2005

Scheme 1

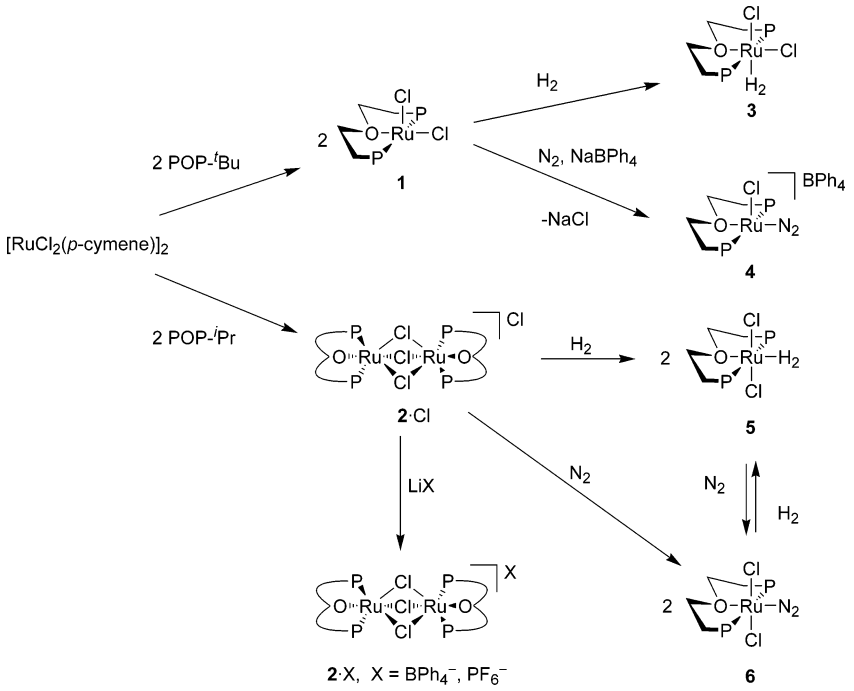

tions with $[RuCl_2(p\text{-cymene})]_2$. The structures of the products and their reactivity toward hydrogen and nitrogen have been investigated. The experimental findings are presented and discussed in the following sections.

Results

Syntheses and Characterization of Bis(2-(dialkylphosphino)ethyl) Ether Ligands. The preparation of bis(2-(di-*tert*-butylphosphino)ethyl) ether (POP-^{t}Bu) was carried out following the literature method.[2g] The synthetic methodology used to prepare POP-^{i}Pr was that employed in the syntheses of other diphosphinoethyl ether ligands[2j] and proceeded by reacting bis(2-chloroethyl) ether with 2 equiv of lithium diisopropylphosphide, which was made in situ from commercially available chlorodiisopropylphosphine and lithium metal.

$$ClP^iPr_2 + 2Li \rightarrow LiP^iPr_2 + LiCl$$

$$2LiP^iPr_2 + (ClCH_2CH_2)_2O \rightarrow ({}^iPr_2PCH_2CH_2)_2O + 2LiCl$$

Both reactions were monitored by $^{31}P\{^1H\}$ NMR and indicated essentially quantitative product formation in solution. POP-^{i}Pr was isolated by distillation as a pyrophoric colorless oil. The POP-^{t}Bu and POP-^{i}Pr ligands were characterized by multinuclear NMR spectroscopy. The spectra of the former were very similar to those reported in the literature.[2g] The latter ligand gave spectra with signals of expected chemical shifts, patterns, and coupling constants (see Experimental Section). A property worth noting in the POP-^{i}Pr ligand is the diastereotopic nature of the methyl groups in each ^{i}Pr substituent. In the NMR spectra, this gave rise to two distinct methyl resonances for the four chemically equivalent ^{i}Pr groups.

Syntheses of Ruthenium Complexes. An outline of synthetic routes developed in this investigation is presented in Scheme 1. Addition of POP-^{t}Bu and POP-^{i}Pr to ruthenium was achieved by substitution of *p*-cymene in $[RuCl_2(p\text{-cymene})]_2$. Heating solutions of $[RuCl_2(p\text{-cymene})]_2$ with 2 equiv of POP-^{t}Bu or POP-^{i}Pr afforded the chlorides $RuCl_2$(POP-^{t}Bu) (**1**) and [(POP-^{i}Pr)Ru(μ-Cl_3)Ru(POP-^{i}Pr)]Cl (**2**·Cl), respectively. Good yields of crystalline material were obtained in both cases. Compound **2**·Cl readily underwent anionic substitution with $LiBPh_4$ or $LiPF_6$ in methanol. The exchange reactions afforded the corresponding salts [(POP-^{i}Pr)Ru(μ-Cl_3)Ru(POP-^{i}Pr)]BPh_4 (**2**·BPh_4) and [(POP-^{i}Pr)Ru(μ-Cl_3)Ru(POP-^{i}Pr)]PF_6 (**2**·PF_6), respectively. Compound **2**·BPh_4 precipitated immediately from the methanol solution, while **2**·PF_6 crystallized slowly over several hours.

No N_2 coordination to ruthenium was observed in solutions of **1**; however H_2 addition to **1** resulted in formation of the dihydrogen complex *cis*,*trans*-Ru(H_2)Cl_2(POP-^{t}Bu) (**3**). The cationic dinitrogen complex [Ru(N_2)Cl(POP-^{t}Bu)]BPh_4 (**4**) was obtained when **1** was reacted with $NaBPh_4$ in CH_2Cl_2 under an atmosphere of nitrogen. An important structural feature of complexes **1** and **4** that is not represented in the simplified drawings of Scheme 1 is C−H···Ru agostic bonding involving a ^{t}Bu group of the POP-^{t}Bu ligand.

(2) (a) Bolzati, C.; Boschi, A.; Uccelli, L.; Tisato, F.; Refosco, F.; Cagnolini, A.; Duatti, A.; Prakash, S.; Bandoli, G.; Vittadin, A. *J. Am. Chem. Soc.* **2002**, *124*, 11468. (b) Buhling, A.; Kamer, P. C. J.; van Leeuwen, P. W. N. M.; Elgersma, J. W.; Goubitz, K.; Fraanje, J. *Organometallics* **1997**, *16*, 3027. (c) Vogl, E. M.; Bruckmann, J.; Kessler, M.; Krüger, C.; Haenel, M. W. *Chem. Ber./Recl.* **1997**, *130*, 1315. (d) Steffey, B. D.; Miedaner, A.; Maciejewski-Framer, M. L.; Bernatis, P. R.; Herring, A. M.; Allured, V. S.; Carperos, V.; DuBois, D. L. *Organometallics* **1994**, *13*, 4844. (e) George, T. A.; Jackson, M. A.; Kaol, B. B. *Polyhedron* **1991**, *10*, 467. (f) George, T. A.; Jackson, M. A. *Inorg. Chem.* **1988**, *27*, 924. (g) Timmer, K.; Thewissen, D. H. M. W.; Marsman, J. W. *Recl. Trav. Chim. Pays-Bas* **1988**, *107*, 248. (h) Thewissen, D. H. M. W.; Timmer, K.; Noltes, J. G.; Marsman, J. W.; Laine, R. M. *Inorg. Chim. Acta* **1985**, *97*, 143. (i) Alcock, N. W.; Brown, J. M.; Jeffery, J. C. *J. Chem. Soc., Dalton Trans.* **1976**, 583. (j) Green, P. T.; Sacconi, L. *J. Chem. Soc. A* **1970**, 866. (j) Sacconi, L.; Gelsomini, J. *Inorg. Chem.* **1968**, *7*, 291.

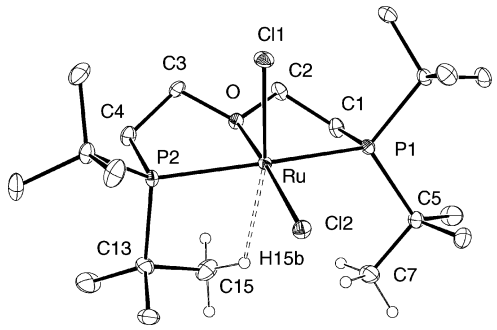

Figure 1. ORTEP and atom-labeling scheme for **1** with the ellipsoids at 30%. Most of the hydrogen atoms are omitted for clarity. Selected bond distances (Å) and angles (deg): Ru−Cl1 2.3505(8), Ru−Cl2 2.3901(7), Ru−O 2.123(2), Ru···H15b 2.23, P1−Ru−P2 161.1(1), P1−Ru−O 82.0(1), P2−Ru−O 80.7(1), Cl1−Ru−Cl2 93.0(1), Cl1−Ru−P1 95.2(1), Cl1−Ru−P2 93.7(1), Cl1−Ru−O 93.6(1), Cl2−Ru−P2 98.7(1), Cl2−Ru−P1 97.5(1), Cl2−Ru−O 173.5(1).

Heating solutions of **2**·Cl under H_2 or N_2 afforded the dihydrogen or dinitrogen complexes, *cis*,*cis*-Ru(H_2)Cl_2(POP-^{i}Pr) (**5**) or *cis*,*cis*-Ru(N_2)Cl_2(POP-^{i}Pr) (**6**), respectively. Interconversion of **5** and **6** could be easily accomplished by degassing and addition of N_2 (**5** → **6**) or H_2 (**6** → **5**) to a solution of the appropriate starting compound. In solutions of **3** and **5** under an atmosphere of D_2, isotopic substitution and formation of the Ru(HD)Cl_2(POP) isotopomers was observed by NMR spectroscopy within minutes at 50 °C. A prolonged exposure to D_2 (>24 h) resulted in the Ru(D_2)Cl_2(POP) isotopomers.

Characterization of Complexes. Complexes **1**, **2**·PF_6, **4**, **5**, and **6** were crystallized, and their molecular structures were determined by X-ray crystallography. All compounds **1**−**6** were characterized by multinuclear NMR spectroscopy and elemental analysis.

Crystal Structure of $RuCl_2$(POP-^{t}Bu) (1). The structure of **1**, shown in Figure 1, confirms the tridentate coordination of the *mer*-POP pincer ligand. The geometry around ruthenium can be considered approximately octahedral with one coordination site occupied by an agostic C−H bond of a ^{t}Bu group. The γ-agostic C15−H15b···Ru interaction is indicated by the geometric parameters of the POP ligand. The Ru−P2−C13 = 101.7(1)° and P2−C13−C15 = 99.8(2)° angles are significantly smaller than the corresponding Ru−P1−C5 = 116.6(1)° and P1−C5−C7 = 106.9(2)° angles, respectively. The Ru−P2 = 2.320(1) Å bond is 0.085 Å shorter than the Ru−P1 = 2.405(1) Å bond due to a contraction in the Ru−P2−C13−C15−H15b cycle. The Ru−C15 separation of 2.845 Å may seem long for an agostic interaction, but precedence has been established and longer C−H···Ru interactions have been observed between a ^{t}Bu group of a P^{t}Bu_2Me ligand and a Ru atom in [Ru{CH=C($SiMe_3$)(Ph)}(CO)(P^{t}Bu_2Me)]$^+$ [Ru···C(agostic) = 3.049 Å][3] and [Ru{(Me_3Si)HC=C−CH=CH($SiMe_3$)}(CO)(P^{t}Bu_2Me)]$^+$ [Ru···C(agostic) = 2.943 Å].[4]

Spectroscopic Characterization of 1 and NMR Evidence for Agostic Interaction. The ambient-temperature ^{1}H NMR spectrum of **1** in CD_2Cl_2 displayed three broad signals (δ 0.99, 2.29, 4.48), whose integration and chemical shifts indicated an assignment of 4 × ^{t}Bu, 2 × PCH_2, and 2 × OCH_2, respectively. The spectra were not consistent with the chiral solid-state structure of **1**, which possesses four unique ^{t}Bu groups and eight unique protons of the CH_2 groups. A combination of four independent processes can explain the room-temperature spectra. One is the inversion of the structure described in Scheme 2 involving chloride ligand exchange that makes the POP plane an effective molecular symmetry plane. Another is the reversible cleavage of the C−H···Ru agostic bonding, as shown in Scheme 3, that results in a time-averaged O−Cl−Cl mirror plane. The third process is rotation of the ^{t}Bu groups, averaging the methyl groups. The fourth process involves the interconversion of the agostic C−H bond with two pendent C−H bonds within the agostic methyl group, i.e., methyl rotation, averaging all three hydrogens.

Scheme 2

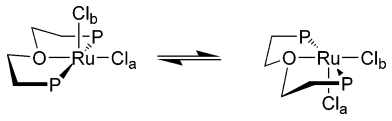

Scheme 3

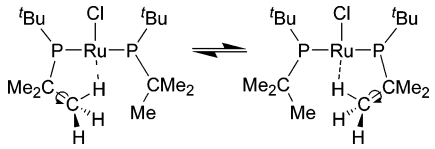

Variable-temperature NMR spectra revealed these processes in a stepwise manner. At −30 °C, the chloride ligand exchange in Scheme 2 became slow. At this temperature the ^{1}H NMR spectrum showed decoalescence of the broad ^{t}Bu signal into two virtual triplets (δ 0.50, 1.40) and decoalescence of the PCH_2 and OCH_2 signals into two multiplets, each with an integration of 4 × 2H. Further lowering the temperature to −110 °C caused decoalescence of the ^{t}Bu resonances into four signals (δ 1.72, 1.58, 1.20, and −2.28) of approximate intensity 6H:12H:12H:6H. The signals were broad and the three downfield signals showed some overlap, but clearly they were due to methyl protons and indicated slow rotation of the ^{t}Bu groups at −110 °C. Specific assignments for the three downfield ^{t}Bu resonances cannot not be made, but the upfield chemical shift of the −2.28 ppm resonance is in agreement with the C−H···Ru agostic interaction present in solution as well as in the crystal. The integration of 6H for this signal is consistent with two dynamic processes still occurring rapidly at the low temperature according to Scheme 3 and involving two methyl groups associated with C7 and C15 in Figure 1: (i) exchange between the agostic CH_3 group and the pendant CH_3 group across the O−Cl−Cl plane and (ii) rotation of the two methyl groups.

Spectroscopic Characterization and Solid-State Molecular Structure of 2. Compound **2**·Cl proved to be insoluble in many organic solvents of varying polarity (hexane, benzene, tetrahydrofuran, and acetone), but it was moderately soluble in CH_2Cl_2 and very soluble in methanol, ethanol, and 2-propanol. These solubility properties provided the first evidence of the ionic nature of the compound. The NMR spectroscopic analysis indicated an asymmetric environment for the POP

(3) Huang, D.; Folting, K.; Caulton, K. G. *J. Am. Chem. Soc.* **1999**, *121*, 10318.
(4) Huang, D.; Oliván, M.; Huffman, J. C.; Eisenstein, O.; Caulton, K. G. *Organometallics* **1998**, *17*, 4700.

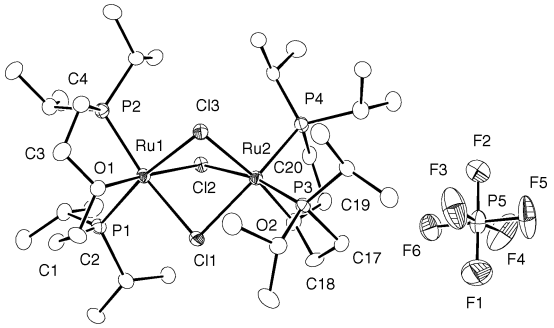

Figure 2. ORTEP and atom-labeling scheme of **2**·PF_6 with thermal ellipsoids at 30%. The hydrogen atoms are omitted for clarity. Selected bond distances (Å) and angles (deg): Ru1−P1 2.284(2), Ru1−P2 2.278(2), Ru2−P3 2.262(2), Ru2−P4 2.289(2), Ru1−O1 2.136(6), Ru2−O2 2.147(6), Cl1−Ru1−Cl2 81.4(1), Cl1−Ru2−Cl2 78.2(1), Cl1−Ru1−Cl3 78.0(1), Cl1−Ru2−Cl3 81.2(1), Cl1−Ru1−P1 90.7(1), Cl1−Ru2−P3 92.0(1), Cl1−Ru1−O1 91.3(2), Cl1−Ru2−O2 91.8(2), Cl2−Ru1−Cl3 82.6(1), Cl2−Ru2−Cl3 82.3(1), Cl2−Ru1−P1 102.1(1), Cl2−Ru1−P2 102.2(1), Cl2−Ru2−P4 88.3(1), Cl2−Ru2−O2 90.0(2), Cl3−Ru1−P1 167.1(1), Cl3−Ru2−P3 101.4(1), Cl3−Ru1−P2 88.7(1), Cl3−Ru2−P4 102.8(1), Cl3−Ru1−O1 89.7(2), Cl3−Ru2−O2 170.6(2), P1−Ru1−P2 101.8(1), P3−Ru2−P4 101.0(1), P1−Ru1−O1 84.3(2), P3−Ru2−O2 85.1(2), P2−Ru1−O1 83.4(2), P4−Ru2−O2 82.5(2).

ligand. The ^{1}H NMR showed three regions of overlapping signals between δ 1.35−1.70, 1.94−2.13, and 3.14−3.4 with integrations of 26H, 4H, and 6H, respectively. The ^{31}P{^{1}H} NMR showed two signals, both doublets of equal coupling, $^2J_{PP}$ = 29.6 Hz, consistent with two inequivalent P^{i}Pr$_2$ groups coordinated in a *cis* fashion to the same ruthenium atom. The ^{13}C{^{1}H} NMR showed eight and four signals for the primary and tertiary carbons of the ^{i}Pr groups, respectively, indicating a unique chemical environment for each ^{i}Pr group. The inequivalence of the two phosphorus groups also resulted in the chemical inequivalence of the two OCH_2 and PCH_2 carbons of the POP ligand. Further NMR analysis of **2** with HETCOR and DEPT allowed detailed assignments to be made (see Experimental Section) but could not further elaborate the structure of the complex.

Attempts to crystallize **2**·Cl were unsuccessful; however, suitable crystals of **2**·PF_6 were obtained and subjected to X-ray analysis. The cation in **2**·PF_6 has a core structure containing two Ru(II) centers and an overall co-facially bioctahedral geometry (Figure 2). The molecule has one symmetrically bridging (Ru1−Cl1 = 2.488(2) Å, Ru2−Cl1 = 2.485(2) Å) and two asymmetrically bridging chloride ligands (Ru1−Cl2 = 2.389(2) Å, Ru2−Cl2 = 2.560(2) Å and Ru1−Cl3 = 2.546(2) Å, Ru2−Cl3 = 2.385(2) Å). For the asymmetric chlorides, the shorter bond is *trans* to oxygen and the longer is *trans* to phosphorus. For example, Cl2 is *trans* to P3 through Ru2 (Cl2−Ru2−P3 = 168.9(1)°) and *trans* to O1 through Ru1 (Cl2−Ru1−O1 = 170.3(1)°). Similar bond angles are observed for Cl3, but Cl1 is *trans* to two phosphorus atoms (Cl1−Ru1−P2 = 165.8(1)° and Cl1−Ru2−P4 = 165.3(1)°); consequently the two Ru−Cl1 separations are identical. These differences result from the much weaker *trans* influence of the coordinated oxygen donor compared to that of the phosphorus. Ignoring the ^{i}Pr groups, **2** has a C_2 axis extending through Cl1 and the midpoint of the Ru−Ru vector. The C_2 operation interchanges the

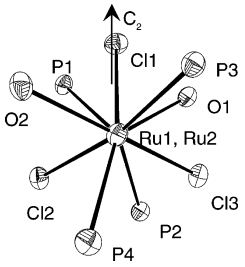

Figure 3. ORTEP view of the cation in **2**·PF_6 showing the C_2 symmetry axis. Carbon and hydrogen atoms are omitted for clarity.

atoms: Ru1 ↔ Ru2, Cl2 ↔ Cl3, P1 ↔ P3, P2 ↔ P4, O1 ↔ O2 (Figure 3). Thus, in solution the chemical equivalence of the two POP ligands is expected. The asymmetry within each POP ligand, as indicated by the NMR spectra, is also evident from the structure in Figure 3.

The question of whether Ru−Ru bonding is present in **2** can be answered by analysis of the Ru−Ru distance. For direct Ru−Ru bonding, the usual range of distances is 2.28−2.95 Å.[5] Elongated Ru−Ru bonds have been reported to be in the range 2.9−3.1 Å,[6] and some very long second-row transition metal−metal bonds have been reported to be as long as 3.2 Å.[7] The Ru−Ru separation in **2**, 3.29 Å, is too long to support any significant metal−metal bonding interaction. It is similar to the Ru−Ru separation (3.44−3.35 Å) in related complexes with a Ru(II)(μ-Cl)$_3$Ru(II) core.[8] Theoretically, there should be no metal−metal bonding in a 36-electron, saturated binuclear complex.

Spectroscopic Characterization of the Dihydrogen Complexes 3 and 5. The ^{1}H NMR spectra of **3** and **5** exhibited one resonance of intensity 2H in the hydride region (δ −10.1, **3**; −14.7, **5**). The resonance of **3** was observed as a triplet with $^2J_{HP}$ = 9 Hz, while that of **5** was a broad singlet ($w_{1/2}$ = 7 Hz). In the region of the phosphine substituents, ^{t}Bu and ^{i}Pr, two resonances were observed which showed the virtual coupling phenomenon characteristic of *trans* P−Ru−P bonding and indicating the meridional coordination mode of the POP ligands. This was supported by a single resonance in the ^{31}P{^{1}H} NMR spectra of both complexes. The ^{1}H spectrum of **3** indicated two chemical environments for the ^{t}Bu groups, while in **5** (with diastereotopic methyl groups) the ^{1}H spectrum pointed to equivalence of all four ^{i}Pr groups. These observations suggested effective C_s and C_{2v} symmetries for the structures of **3** and **5**, respectively, according to Scheme 1. The ^{1}H NMR data for the PCH_2 and OCH_2 groups, along with the ^{13}C{^{1}H} NMR data, were consistent with these conclusions.

Estimates of the H−H Distance in 3 and 5 in Solution (T_{1min} and J_{HD}). To further characterize the dihydrogen ligands in **3** and **5**, we obtained estimates

(5) (a) Dekleva, T. W.; Thorburn, I. S.; James, B. R. *Inorg. Chim. Acta* **1985**, *100*, 49. (b) Mattson, B. M.; Heiman, J. R.; Pignolet, L. H. *Inorg. Chem.* **1976**, *15*, 564. (c) Schumann, H.; Opitz, J.; Pickardt, J. *J. Organomet. Chem.* **1977**, *128*, 253. (d) Jones, R. A.; Wilkinson, G.; Coloquohoun, I. J.; McFarlane, W.; Galas, A. M. R.; Hursthouse, M. B. *J. Chem. Soc., Dalton Trans.* **1980**, 2480.

(6) (a) Keijsper, J.; Polm, L. H.; van Koten, G.; Vrieze, K.; Seignette, P. F. A. B.; Stam, C. H. *Inorg. Chem.* **1985**, *24*, 518. (b) Carty, A. J.; MacLaughlin, S. A.; van Wagner, J.; Taylor, N. J. *Organometallics* **1982**, *1*, 1013.

(7) Dahl, L. F.; Wampler, D. L. *J. Am. Chem. Soc.* **1959**, *81*, 3150.

(8) Seddon, E. A.; Seddon, K. R. *The Chemistry of Ruthenium*; Elsevier: Amsterdam, 1984; pp 310, 487−515.

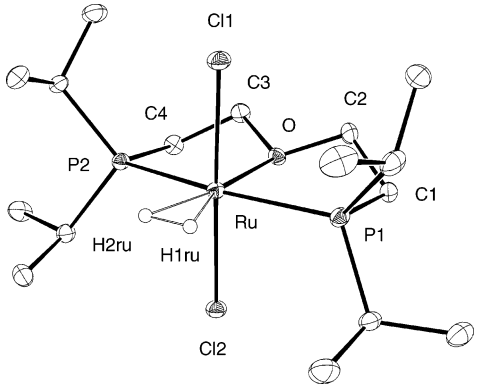

Figure 4. Crystal structure of **5** with the ellipsoids at 30%. Most of the hydrogen atoms are removed for clarity. Selected bond distances (Å) and angles (deg): Ru−P1 2.350(1), Ru−Cl1 2.4093(9), Ru−Cl2 2.4076(8), Ru−O 2.167(2), Ru···H1ru, H2ru 1.67(2), H1ru−H2ru 0.90, P1−Ru−P2 163.46(4), P1−Ru−O 81.74(7), Cl1−Ru−Cl2 177.08(3), Cl1−Ru−P1 91.60(3), Cl1−Ru−O 89.87(6), Cl2−Ru−P1 88.04(3), Cl2−Ru−O 87.21(6).

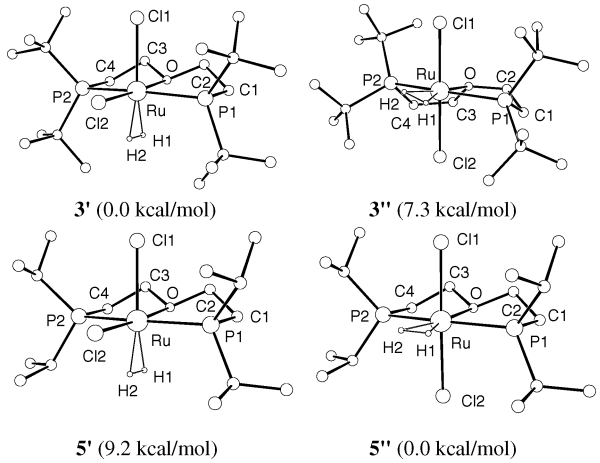

Figure 5. Theoretical structures of complexes **3** and **5**. The ZPE-corrected energies are relative to the more stable isomer in each pair.

of the H−H distances by measuring the T_{1min} (minimum spin−lattice relaxation times) of the H_2 resonances along with the J_{HD} (H−D coupling constants) of the monodeuterated isotopomers Ru(HD)Cl_2(POP-^{t}Bu) (**3-*d***) and Ru(HD)Cl_2(POP-^{i}Pr) (**5-*d***). The T_{1min} times for **3** and **5** were found to be 16.1 and 14.6 ms, respectively, at −55 °C (300 MHz, toluene-d_8), Using the methodology of Halpern and co-workers we calculated the H−H separations of 1.13 Å in **3** and 1.11 Å in **5**.[9] No correction for rapid H_2 spinning has been applied in these calculations because of the computational evidence (see below) indicating that the H_2 ligands of **3** and **5** are undergoing 2-fold reorientation that should have no effect on the T_1.[10] The J_{HD} couplings in **3-*d*** and **5-*d*** are 27.0 and 27.3 Hz, respectively, and these values correspond to H−H separations of 1.00 Å in **3** and 0.99 Å in **5**.[11]

Solid-State Molecular Structure of 5. The dihydrogen complex **5** was crystallized and characterized by X-ray diffraction. The crystallographic results are presented in Figure 4. The crystal structure is in agreement with the structure deduced from the NMR data in solution, where **5** is expected to have an effective C_{2v} symmetry due to a combination of rapid rotation of the ^{i}Pr groups and conformational nonrigidity of the POP ligand backbone. Although complex **3** was also crystallized, crystallographic determination of its molecular structure was unsuccessful due to disorder problems.

Theoretical Structures of 3 and 5. To better understand structural preferences in the system of complexes **3** and **5**, we carried out a series of DFT calculations and optimized four geometries presented in Figure 5 possessing the dihydrogen ligand *trans* to chloride (**3′** and **5′**) or *trans* to oxygen (**3″** and **5″**). For Ru(H_2)Cl_2(POP-^{i}Pr), the more stable isomer **5″** has the structure closely resembling the crystal structure of **5**, with the differences within 0.03 Å and 2° for the bond distances and angles, respectively. Isomer **5′**, possessing H_2 *trans* to a chloride, is 9.2 kcal/mol less stable than **5″**. The higher stability of **5″** over **5′** is probably due to somewhat stronger bonding of the H_2 *trans* to a weak donor oxygen atom in **5″**, which manifests in the slightly longer H−H distance of 0.925 Å in **5″** versus 0.907 Å in **5′**. It is however difficult to say whether this effect is due to stronger σ-bonding (H_2→Ru) or better back-bonding (H_2←Ru), or a combination of both.

In the system of Ru(H_2)Cl_2(POP-^{t}Bu) the structural preferences are reversed and the C_s symmetrical isomer **3′** is 7.3 kcal/mol more stable than the approximately C_{2v} symmetrical **3″**, in agreement with the solution NMR data for **3**. The main difference between **3** and **5** is the size of the groups on phosphorus, and the *trans*-dichloride structure **3″** is disfavored for steric reasons. The steric problems in **3″** become obvious at once when the C−H hydrogens of the ^{i}Pr groups in **5″** are replaced by methyls, because this brings two CH_3 groups within 1.40 Å of Cl2. To avoid such close contacts, the P^{t}Bu$_2$ groups had to move during the DFT optimization of **3″**, which resulted in a distorted POP ligand backbone with the P1−C1 and P2−C4 bonds rotated out of the POP plane. We have earlier commented[12] on the structure of related ruthenium complexes derived from 1,5-bis(di-*tert*-butylphosphino)pentane and explained their preference for square-pyramidal geometry by the steric requirements of the ^{t}Bu$_2$ groups, two of which occupy one coordination site, limiting the coordination number to five. A similar situation is seen in **1**, where the structure is furthermore stabilized by agostic bonding.

In **3′** and **5″**, the dihydrogen ligand is aligned along the O−Cl2 and P1−P2 axes, respectively. For these two complexes we studied the process of H_2 rotation around the Ru−H_2 bond. Single transition-state structures were found, **3′ts** and **5″ts**, with the relative energies of 0.9 and 0.7 kcal/mol above **3′** and **5″**, respectively. These energy barriers are very low and, in solution, the H_2 reorientation should be fast on the time scale of molecular tumbling. In both transition-state geometries the coordinated H_2 is rotated by 90° relative to the ground-state orientation; that is, the H−H is coplanar with P1

(9) Desrosiers, P. J.; Cai, L.; Lin, Z.; Richards, R.; Halpern, J. *J. Am. Chem. Soc.* **1991**, *113*, 4173.

(10) (a) Zilm, K. W.; Millar, J. M. *Adv. Magn. Opt. Reson.* **1990**, *15*, 163. (b) Gusev, D. G.; Kuhlman, R. L.; Renkema, K. B.; Eisenstein, O.; Caulton, K. G. *Inorg. Chem.* **1996**, *35*, 6775. (c) Facey, G. A.; Fong, T. P.; Gusev, D.; Macdonald, P. M.; Morris, R. H.; Schlaf, M.; Xu, W. *Can. J. Chem.* **1999**, *77*, 1899.

(11) (a) Gusev, D. G. *J. Am. Chem. Soc.* **2004**, *126*, 14249. (b) Calculated using eq 3 from ref 11a.

(12) Gusev, D. G.; Lough, A. J. *Organometallics* **2002**, *21*, 5091.

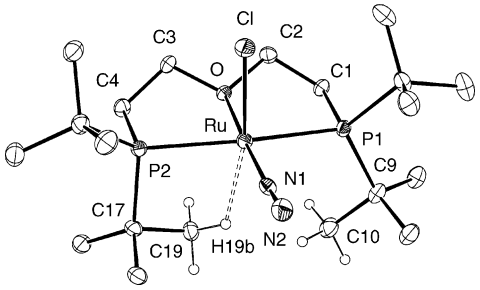

Figure 6. ORTEP and atom-labeling scheme of the cation in **4** with the ellipsoids at 30%. Most of the hydrogen atoms are omitted for clarity. Selected bond distances (Å) and angles (deg): Ru−Cl 2.337(1), Ru−O 2.117(3), Ru−N1 1.946(3), N1−N2 1.054(5), Ru···H19b 2.08, P1−Ru−P2 162.81(4), P1−Ru−O 81.87(7), P2−Ru−O 82.39(7), Cl−Ru−N1 88.2(1), Cl−Ru−P1 95.21(4), Cl−Ru−P2 91.62(4), Cl−Ru−O 89.78(8), N1−Ru−P1 97.0(1), N1−Ru−P2 99.0(1), N1−Ru−O 177.6(1), Ru−N1−N2 175.2(4).

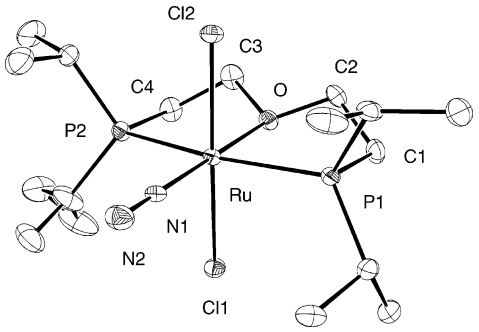

Figure 7. ORTEP and atom-labeling scheme of **6** with the ellipsoids at 30%. The hydrogen atoms are omitted for clarity. Selected bond distances (Å) and angles (deg): Ru−Cl1 2.395(1), Ru−O 2.147(3), Ru−Cl2 2.420(1), Ru−N1 1.893(3), Ru−P1 2.368(1), P1−Ru−P2 163.8(1), Cl1−Ru−Cl2 176.8(1), O−Ru−N1 179.7(1), Cl1−Ru−P1 89.8(1), Cl1−Ru−N1 90.6(1), Cl1−Ru−O 89.2(8), Cl2−Ru−P1 90.4(1), Cl2−Ru−N1 92.5(1), Cl2−Ru−O 87.7(1), P1−Ru−O 81.8(1), P1−Ru−N1 98.4(1), N2−N1−Ru, 179.3(3).

and P2 in **3′ts** and is coplanar with Cl1 and Cl2 in **5″ts**. Thus, the intramolecular reorientation of the dihydrogen ligand around the Ru−H_2 bond comprises 2-fold jumps rather than a continuous spinning.

The calculated r(H−H) = 0.93 Å is the same in **3′** and **5″** and is shorter than the experimental values of 1.00 Å in **3** and 0.99 Å in **5** derived from the J_{HD} couplings, which in turn are shorter than the distances determined from the T_{1min} relaxation times. These differences are natural because the theoretical H−H distances correspond to electronic minimums, whereas the values obtained by experimental means can be to a different degree affected by anharmonic vibrations of the hydrogen atoms[13] and, for dihydrogen complexes, systematically appear longer than the distances from DFT calculations.[11]

Solid-State Molecular Structure and Spectroscopic Characterization of 4 and 6. These two species provide another example of the dramatic difference the substituents on phosphorus make for the stability and structure of the POP pincer complexes. After establishing in the preceding section that the vacant site in the pyramidal *cis*-$RuCl_2$(POP-^{t}Bu) fragment is unfavorable for steric reasons, the lack of dinitrogen coordination to **1**, and so the instability of *cis*,*trans*-Ru(N_2)Cl_2(POP-^{t}Bu), come as no surprise. It is interesting, however, that a dinitrogen complex could be made from **1** in the presence of $NaBPh_4$, via substitution of a chloride ligand. An elemental analysis of the product crystallized from dichloromethane confirmed the composition, [Ru(N_2)Cl(POP-^{t}Bu)]BPh_4·CH_2Cl_2 (**4**). A strong peak was observed in the IR spectrum of **4** due to the N≡N stretch at 2143 cm^{-1}. Finally, a crystal structure of **4** was determined, which provided important structural details.

The structure of the cation in **4** is shown in Figure 6 and closely resembles that of the parent compound **1** in Figure 1. Except for the dinitrogen ligand that replaced a chloride, **4** appears identical with **1** and likewise features agostic bonding of a ^{t}Bu group. This γ-agostic C19−H19b···Ru interaction makes **4** asymmetric. The Ru−P2−C17 = 98.0(1)° and P2−C17−C19 = 99.7(3)° angles are smaller than the corresponding Ru−P1−C9 = 117.6(1)° and P1−C9−C10 = 107.8(3)° angles, respectively. The Ru−P2 = 2.340(1) Å bond is 0.093 Å shorter than the Ru−P1 = 2.433(1) Å bond due to a contraction in the Ru−P2−C17−C19−H19b cycle. After comparing these data with the corresponding geometrical parameters in **1**, it appears that the degree of contraction is slightly greater in **4**. The agostic Ru−C19 separation is also slightly shorter in **4**: 2.740 Å versus the 2.845 Å Ru−C15 distance in **1**. This C−H···Ru agostic bonding persists in **4** in solution. Above −60 °C, the ^{1}H NMR spectra of **4** showed two 1:1 resonances due to ^{t}Bu groups at δ 1.44 and 0.40. The latter became very broad at −60 °C and decoalesced at −80 °C to give one broad peak of intensity 12H between δ 1.1−1.5 and another of intensity 6H at δ −1.9 ppm. At −100 °C, the ^{t}Bu region of the proton spectrum of **4** looked very similar to that of **1**. Obviously the dynamic process proposed in Scheme 3 operates in both compounds at −100 °C.

We next turn our attention to the dinitrogen complex Ru(N_2)Cl_2(POP-^{i}Pr) (**6**), whose formation is in accord with the existence of the analogous dihydrogen complex Ru(H_2)Cl_2(POP-^{i}Pr) (**5**). Notwithstanding the absence of a hydride resonance, the ^{1}H and ^{13}C{^{1}H} NMR spectra of **6** were very similar to those of **5**. In addition, the IR spectrum of **6** showed a very strong ν(N≡N) absorbance at 2119 cm^{-1}, a frequency lower than ν(N≡N) = 2143 cm^{-1} for the cationic **4**, as expected. These results indicated a structure depicted in Scheme 1 similar to that observed for **5** except with a N_2 ligand in place of the H_2 ligand. Confirmation was provided by an X-ray crystallographic analysis, the results of which are presented in Figure 7.

The structure of **6** is octahedral with the POP ligand in a pincer coordination mode. It shows two *trans* chlorides and a η^1-N_2 ligand *trans* to the oxygen atom. There is some disorder in one ^{i}Pr group (C16 and C16A), but otherwise the structure is well defined. The most notable feature of **6** is the dinitrogen ligand. The N−N separation is 1.101(5) Å and is not statistically different from the corresponding separation in free N_2 (1.0975 Å). Thus the dinitrogen ligand in **6** is only marginally activated.[14] Other known pincer complexes of ruthenium show weak activation of coordinated dinitrogen and

(13) Heinekey, D. M.; Lledós, A.; Lluch, J. M. *Chem. Soc. Rev.* **2004**, *33*, 175.

Scheme 4

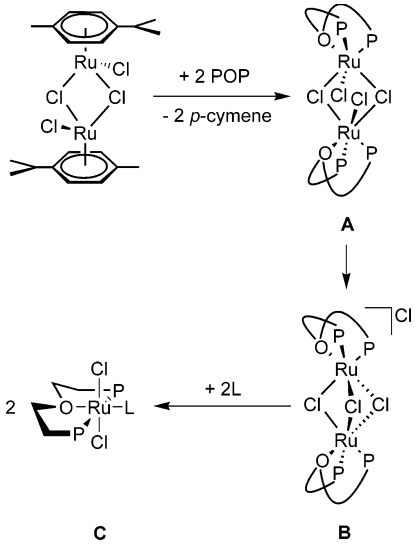

have a propensity to undergo ligand substitution at the N_2 site.[15,16] The N_2 ligand in **6** also displays this reactivity and is easily displaced by H_2. After 1 h at room temperature a benzene solution of **6**, which was placed under a H_2 atmosphere, began to show the characteristic resonances of **5** in the ^1H and $^{31}P\{^1H\}$ NMR spectra. Full conversion of **6** to **5** was accomplished by repeated degas and H_2 backfill cycles. This conversion is reversible, i.e., **5** to **6**, by several degas and N_2 backfill cycles (Scheme 1).

Discussion

Several times in this investigation we have seen that the chemistry of POP complexes is strongly influenced by the steric demand of the substituents on phosphorus. The reaction of $[RuCl_2(p\text{-cymene})]_2$ and POP-^{t}Bu yielded the *mer*-POP complex **1**, while the reaction of POP-^{i}Pr afforded the dimer **2** with two *fac*-POP ligands. Formation of **1** and **2** might proceed by a similar mechanism depicted in Scheme 4. In the first step, 2 equiv of POP displace *p*-cymene in $[RuCl_2(p\text{-cymene})]_2$ to form a short-lived intermediate, $Ru_2(\mu\text{-}Cl)_2Cl_2(POP)_2$ (**A**). In the next step, Cl^- dissociates from **A** to afford $[Ru_2(\mu\text{-}Cl)_3(POP)_2]$-Cl (**B**), which was isolated in the case of the POP-^{i}Pr ligand. The last step involves the reaction of **B** with H_2 or N_2 to form **C**. In the case of POP-^{t}Bu, the larger ^{t}Bu substituents strongly destabilize the hypothetical dimers **A** and **B**, which dissociate to give **1**.

Another demonstration of the role of phosphine substituents in the chemistry of POP pincer complexes is the difference in the structure of **3** and **5**. In **5**, the H_2 ligand is *trans* to the oxygen in the equatorial plane (defined as the POP plane), while in **3**, the H_2 ligand occupies the most crowded axial site. Two properties of H_2 ligand, compared to chloride, make it the more favorable ligand for a crowded environment. First, H_2 is smaller than chloride. A qualitative estimate of the relative sizes of η^2-H_2 and chloride ligands may be obtained if it is assumed that the steric profile of each ligand is circular from the perspective of the metal center and radiates out from the center of the ligand to the limit of the van der Waals radius. The size of a chloride is then 1.8 Å, i.e., its van der Waals radius.[17] The size of the η^2-H_2 ligands in **3** and **5** is estimated to be 1.7 Å, which is arrived at by adding one-half the H−H bond distance (0.5 Å) to the van der Waals radius of hydrogen (1.2 Å).[17] By these estimates, even along its longest axis the H_2 ligand is smaller than chloride. The effective size of coordinated dihydrogen is even smaller in the direction perpendicular to the H−H bond, and the ligand can rotate away from bulky groups. The second factor that influences the amount of steric interaction with the ^{t}Bu substituents in **3** and **5** is the bond length. In these complexes, the Ru−H and Ru−Cl distances compare as ca. 1.63 and 2.42 Å, respectively. This places the H_2 ligand much closer to ruthenium and away from the ^{t}Bu substituents, as illustrated in Chart 3.

Chart 3

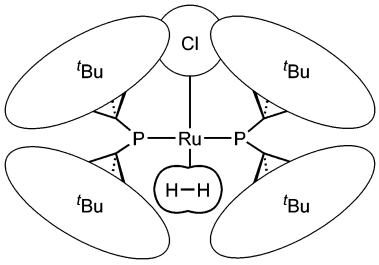

The dinitrogen complexes obtained in this investigation further demonstrated the influence of the bulky ^{t}Bu substituents. Compound **2** reacted with N_2 to give **6**, yet **1** did not react with N_2 to form an analogous compound, nor did **3** substitute N_2 for H_2. An argument similar to that presented above can rationalize these observations. The Ru−N1 bond in **6** is 1.89 Å and the Ru−N2 distance is 2.99 Å. This would place an N_2 ligand, if it were coordinated at the axial site in **1**, in an area occupied by the ^{t}Bu groups, much like the chloride in Chart 3. The isolation of the cationic dinitrogen species $[Ru(N_2)Cl(POP\text{-}^tBu)]^+$ (**4**) via substitution of a chloride in **1** decisively demonstrated that the lack of N_2 coordination to **1** could not be due to an electronic effect.

There is another important structural aspect of the chemistry of the pincer ligands that should be discussed. Milstein and co-workers have recently reported a reaction of $RuCl_2(PPh_3)_3$ and PNP-^{t}Bu (PNP-^{t}Bu = 2,6-bis(di-*tert*-butylphosphinomethyl)pyridine) in THF that afforded a mixture of $RuCl_2(N_2)$(PNP-^{t}Bu) and a dinitrogen-bridged dimer complex, $Ru_2Cl_4(\mu\text{-}N_2)$(PNP-^{t}Bu)$_2$, shown in Scheme 5.[18] The two products existed in equilibrium dependent on the concentration of the complex and the amount of N_2 in the system. Under a nitrogen atmosphere, the equilibrium favored the dimer complex by a factor of 10:1. Under an argon purge, nearly all of the monomer was transformed into the dimer.

(14) (a) MacKay, B. A.; Fryzuk, M. D. *Chem. Rev.* **2004**, *104*, 385. (b) Fryzuk, M. D.; Johnson, S. A. *Coord. Chem. Rev.* **2000**, *200−202*, 379.

(15) Gusev, D. G.; Dolgushin, F. M.; Antipin, M. Y. *Organometallics* **2000**, *19*, 3429.

(16) (a) del Río, I.; Back, S.; Hannu, M. S.; Rheinwald, G.; Lang, H.; van Koten, G. *Inorg. Chim. Acta* **2000**, *300−302*, 1094. (b) del Río, I.; Gossage, R. A.; Hannu, M. S.; Lutz, M.; Spek, A. L.; van Koten, G. *Organometallics* **1999**, *18*, 1097.

(17) Pauling, L. *The Nature of the Chemical Bond*, 3rd ed.; Cornell University Press: Ithaca, 1960.

(18) Zhang, J.; Gandelman, M.; Shimon, L. J. W.; Rozenberg, H.; Milstein, D. *Organometallics* **2004**, *23*, 4026.

Scheme 5

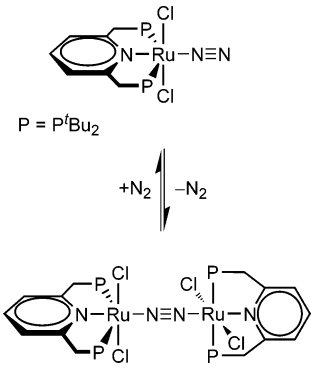

Chart 4. View along the N−Ru and O−Ru Axis in RuCl$_2$(POP-^{t}Bu) (A) and RuCl$_2$(PNP-^{t}Bu) (B)

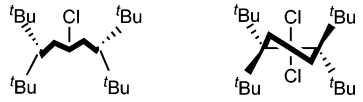

Chart 5. Side Views of RuCl$_2$(POP-^{t}Bu) (A) and RuCl$_2$(PNP-^{t}Bu) (B)

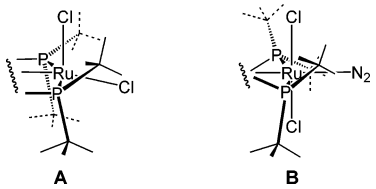

It is interesting that these complexes are stable and yet the analogous POP complexes, RuCl$_2$(N$_2$)(POP-^{t}Bu) or Ru$_2$Cl$_4$(μ-N$_2$)(POP-^{t}Bu)$_2$, are not. Conversely, it is curious that the POP-^{t}Bu pincer compound **1** was isolated and yet Milstein et al. did not observe an analogous compound RuCl$_2$(PNP-^{t}Bu). The differing factor between these complexes is the pincer ligand backbone. In **1**, the ether linkage is well aligned along the POP plane (structure **A** in Chart 4). In complexes **3**−**6** the fused five-membered rings of the coordinated POP ligands are coplanar. On the contrary, the solid-state molecular structure of Ru$_2$Cl$_4$(μ-N$_2$)(PNP-^{t}Bu)$_2$ (**B** in Chart 4)[18] shows the pyridine ring rotated out of the PNP plane by about 26° and has one CH$_2$ group above and the other below the equatorial plane of the molecule. It appears that these differences can be due to conformational preferences of the ligands. An inspection of 124 crystal structures in the Cambridge Structural Database of complexes with PNP and PCP pincer ligands containing an aromatic ring in the backbone found that two-thirds of them have the aromatic ring rotated with respect to the ligand plane.

In the case of complexes **1** and **3**−**6**, the PR$_2$ groups are in an eclipsed conformation as in **A** in Chart 5. In **1**, this arrangement places two ^{t}Bu substituents in the vacant coordination site and makes it unfavorable for coordination of even small ligands such as N$_2$ or Cl. The twisted backbone of the PNP-^{t}Bu system causes a *gauche* conformation of the two P^{t}Bu$_2$ groups, as schematically shown in **B** in Chart 5. In this case, the ^{t}Bu$_2$ groups are more evenly spread between the ligands that eases the repulsion. It can be said that the POP-^{t}Bu ligand has conformational properties that make it an effectively more bulky ligand than the related PNP-^{t}Bu system.

Experimental Section

All manipulations were preformed under nitrogen in a drybox or under argon using standard Schlenk techniques. All solvents were purchased anhydrous and were stored and dispensed in a drybox. Deuterated solvents were deoxygenated and dried by standard methods.[19] NMR spectra were recorded on a Varian Unity Inova 300 NMR spectrometer. Spin−lattice relaxation times T_1 were determined as a function of temperature by the inversion−recovery method. Infrared spectra were recorded on a Perkin-Elmer Spectrum BX FT-IR spectrometer. Preparation of [RuCl$_2$(*p*-cymene)]$_2$ was preformed as described in the literature.[20] Bis(2-(di-*tert*-butylphosphino)ethyl) ether was prepared according to literature methods.[2g] Gaseous D$_2$ (99.8%), lithium metal pellets, chlorodiisopropylphosphine, and bis(2-chloroethyl) ether were purchased from Aldrich and used without further purification.

Preparation of Lithium Diisopropylphosphide. A tetrahydrofuran solution (20 mL) of ^{i}Pr$_2$PCl (10.0 g, 65.6 mmol) was added dropwise over a period of approximately 20 min to a stirred suspension of lithium metal pellets (1.03 g, 149 mmol) in tetrahydrofuran (50 mL). The mixture was stirred for approximately 48 h. The solution was filtered to remove excess lithium, and the product was used without further purification.

Preparation of Bis(2-(diisopropylphosphino)ethyl) Ether (POP-^{i}Pr). A tetrahydrofuran (15 mL) solution of (ClCH$_2$CH$_2$)$_2$O (4.69 g, 32.8 mmol) was added to a cooled and stirred tetrahydrofuran (70 mL) solution of LiP^{i}Pr$_2$ (8.14 g, 65.6 mmol) dropwise over a period of 30 min. The temperature of the mixture was kept between −20 and −30 °C. The solution was stirred at ambient temperature for 1 h. The solvent was removed and the residue dried in vacuo for 30 min. Hexane (40 mL) was added to the residue, and the mixture was washed with water (3 × 20 mL). The product was purified by fractional distillation under reduced pressure (0.01 mmHg). Bis(2-(diisopropylphosphino)ethyl) ether was obtained as a pyrophoric colorless oil. Yield: 5.26 g (52%). ^{1}H NMR (C$_6$D$_6$): δ 0.99 (m, 24H, PC(C*H*$_3$)$_2$), 1.57 (dqq, $^2J_{HP}$ = 2.0 Hz, $^2J_{HH}$ = 7.0 Hz, $^2J_{HH}$ = 7.0 Hz, 4H, PC*H*), 1.72 (m, 4H, PC*H*$_2$), 3.63 (m, 4H, OC*H*$_2$). ^{31}P{^{1}H} NMR (C$_6$D$_6$): δ −1.3 (s). ^{13}C{^{1}H} NMR (C$_6$D$_6$): δ 19.2 (d, $^2J_{CP}$ = 9.7 Hz, PC*C*H$_3$), 20.6 (d, $^1J_{CP}$ = 17.0 Hz, PC*C*H$_3$′), 23.5 (d, $^1J_{CP}$ = 19.8 Hz, P*C*H$_2$), 24.0 (d, $^2J_{CP}$ = 13.6 Hz, P*C*H), 71.1 (d, $^2J_{CP}$ = 31.7 Hz, O*C*H$_2$).

Preparation of RuCl$_2$\{(^{t}Bu$_2$PCH$_2$CH$_2$)$_2$O\} (1). A stirred mixture of [RuCl$_2$(*p*-cymene)]$_2$ (626 mg, 1.02 mmol) and (^{t}Bu$_2$PCH$_2$CH$_2$)$_2$O (775 mg, 2.14 mmol) in 15 mL of toluene was heated to 90 °C for 23 h. The mixture was cooled to ambient temperature for a period of 1 h. The solid product was filtered, washed with toluene (3 × 3 mL), and dried in vacuo. Yield: 785 mg (72%). Anal. Calcd for C$_{20}$H$_{44}$Cl$_2$OP$_2$Ru: C, 44.94; H, 8.29. Found: C, 44.52; H, 8.12. ^{1}H NMR (CD$_2$Cl$_2$, 243 K): δ 0.50 (vt, ^vJ = 11.4 Hz, 18H, PC(C*H*$_3$)$_3$), 1.40 (vt, ^vJ = 12.9 Hz, 18H, PC(C*H*$_3$)$_3$), 2.19 (m, 2H, PC*H*$_2$), 2.37 (m, 2H, PC*H*$_2$), 3.92 (m, 2H, OC*H*), 4.31 (m, 2H, OC*H*). ^{31}P{^{1}H} NMR (CD$_2$Cl$_2$, 243 K): δ 17.7 (s). ^{13}C{^{1}H} NMR (CD$_2$Cl$_2$, 243 K): δ 20.6 (vt, ^vJ = 11.5 Hz, P*C*H$_2$), 27.7 (s, PC(*C*H$_3$)$_3$), 29.0 (s, PC(*C*H$_3$)$_3$), 35.2 (vt, ^vJ = 10.0 Hz, P*C*(CH$_3$)$_3$), 38.0 (vt, ^vJ = 14.6 Hz, P*C*(CH$_3$)$_3$), 76.9 (vt, ^vJ = 13.9 Hz, O*C*H$_2$).

RuCl$_2$\{(^{t}Bu$_2$PCH$_2$CH$_2$)$_2$O\} is a green crystalline solid. It has good solubility in dichloromethane but is much less soluble in tetrahydrofuran, benzene, or toluene. In solid form the compound is stable in air for 24 h or more, but the compound is very air sensitive in solution.

(19) Perrin, D. D.; Armarego, W. L. F. *Purification of Laboratory Chemicals*, 3rd ed.; Pergamon: New York, 1988.
(20) Bennett, M. A.; Huang, T. N.; Matheson, T. W.; Smith, A. K. *Inorg. Synth.* **1981**, *21*, 74.

Preparation of [Ru$_2$(μ-Cl)$_3${(^{i}Pr$_2$PCH$_2$CH$_2$)$_2$O}$_2$]Cl (2). A stirred mixture of [RuCl$_2$(*p*-cymene)]$_2$ (655 mg, 1.07 mmol) and (^{i}Pr$_2$PCH$_2$CH$_2$)$_2$O (659 mg, 2.15 mmol) in 12 mL of methanol was heated to 65 °C for 48 h. The solvent was removed in vacuo, and 12 mL of toluene was added to the residue. On standing for several hours an orange powder precipitated from solution. The solid was filtered, washed with toluene (3 × 3 mL), and dried in vacuo. The supernatant was placed in a −28 °C freezer overnight, and a second crop of crystals was collected. Yield: 708 mg (70%). ^{1}H NMR (CD$_3$OD): δ 1.35−1.70 (m, 52H, 48H from PCC*H*$_3$ and 4H from PC*H*$_2$), 1.94 (m, 2H, PC*H*$_2$), 2.13 (m, 6H, 4H from PC*H* and 2H from PC*H*$_2$), 3.1−3.4 (m, 6H, 4H from PC*H* and 2H from OC*H*$_2$), 3.5−3.8 (m, 4H, OC*H*$_2$), 3.95 (m, 2H, OC*H*$_2$). ^{31}P{^{1}H} NMR (CD$_3$OD): δ 64.8 (d, $^2J_{PP}$ = 29.6 Hz), 72.5 (d, $^2J_{PP}$ = 29.6 Hz). ^{13}C{^{1}H} NMR (CD$_3$OD): δ 19.16 (d, $^2J_{CP}$ = 8.4 Hz, PC*C*H$_3$), 19.80 (d, $^2J_{CP}$ = 5.5 Hz, PC*C*H$_3$), 20.60 (d, $^2J_{CP}$ = 2.4 Hz, PC*C*H$_3$), 20.79 (d, $^2J_{CP}$ = 5.2 Hz, PC*C*H$_3$), 21.06 (s, PC*C*H$_3$), 21.16 (s, PC*C*H$_3$), 21.29 (s, PC*C*H$_3$), 20.46 (s, PC*C*H$_3$), 26.61 (d, $^1J_{CP}$ = 23.9 Hz, P*C*H$_2$), 28.37 (d, $^1J_{CP}$ = 23.9 Hz, P*C*H), 29.99 (d, $^1J_{CP}$ = 21.9 Hz, P*C*H), 30.08 (d, $^1J_{CP}$ = 16.1 Hz, P*C*H$_2$), 31.11 (d, $^1J_{CP}$ = 19.0 Hz, P*C*H), 33.06 (d, $^1J_{CP}$ = 23.3 Hz, P*C*H), 77.68 (s, O*C*H$_2$), 79.29 (s, O*C*H$_2$).

[Ru$_2$(μ-Cl)$_3${(^{i}Pr$_2$PCH$_2$CH$_2$)$_2$O}$_2$]Cl is an orange powder that has good solubility in methanol, ethanol, and 2-propanol, fair solubility in 3-methyl-1-butanol, but is insoluble in acetone, tetrahydrofuran, 2-methyl-2-propanol, 2-methyl-2-butanol, dichloromethane, and nonpolar solvents such as hexane, benzene, and toluene. The compound is stable in air for several days in solid form but air sensitive in solution.

Preparation of [Ru$_2$(μ-Cl)$_3${(^{i}Pr$_2$PCH$_2$CH$_2$)$_2$O}$_2$}][BPh$_4$] (2·BPh$_4$). A 2.5 mL methanol solution of LiBPh$_4$·3CH$_3$OCH$_2$-CH$_2$OCH$_3$ (125 mg, 0.210 mmol) was added dropwise to a stirred methanol (5 mL) solution of [Ru$_2$(μ-Cl)$_3${(^{i}Pr$_2$PCH$_2$-CH$_2$)$_2$O}$_2$}]Cl (201 mg, 0.210 mmol). An orange precipitate immediately formed. The mixture was stirred for an additional 10 min. The precipitate was collected via filtration and washed with methanol (3 × 3 mL). Yield: 223 mg (86%). Anal. Calcd for C$_{56}$H$_{92}$BCl$_3$O$_2$P$_4$Ru$_2$: C, 54.22; H, 7.47. Found: C, 53.92; H, 7.42. ^{1}H NMR (thf-d_8): δ 1.26−1.64 (m, 54H), 2.01 (m, 6H), 2.92−3.53 (m, 10H), 3.71−3.85 (m, 2H), 6.71 (m, 4H, C$_6$H$_5$), 6.85 (m, 8H, C$_6$H$_5$), 7.28 (m, 8H, C$_6$H$_5$). ^{31}P{^{1}H} NMR (thf-d_8): δ 64.7 (d, $^2J_{PP}$ = 29.1 Hz), 73.5 (d, $^2J_{PP}$ = 29.1 Hz). ^{13}C{^{1}H} NMR (thf-d_8): δ 19.14 (d, $^2J_{CP}$ = 8.4 Hz, PC*C*H$_3$), 19.81 (d, $^2J_{CP}$ = 7.2 Hz, PC*C*H$_3$), 20.52 (d, $^2J_{CP}$ = 3.7 Hz, PC*C*H$_3$), 20.62 (d, $^2J_{CP}$ = 6.0 Hz, PC*C*H$_3$), 20.98 (d, $^2J_{CP}$ = 3.2 Hz, PC*C*H$_3$), 21.03 (d, $^2J_{CP}$ = 1.7 Hz, PC*C*H$_3$), 21.24 (s, PC*C*H$_3$), 21.47 (s, PC*C*H$_3$), 26.22 (d, $^1J_{CP}$ = 23.6 Hz, P*C*H$_2$), 28.17 (d, $^1J_{CP}$ = 23.6 Hz, P*C*H), 29.97 (d, $^1J_{CP}$ = 21.3 Hz, P*C*H), 30.00 (d, $^1J_{CP}$ = 24.4 Hz, P*C*H$_2$), 30.79 (d, $^1J_{CP}$ = 18.4 Hz, P*C*H), 32.86 (d, $^1J_{CP}$ = 23.0 Hz, P*C*H), 77.13 (s, O*C*H$_2$), 78.96 (s, OCH$_2$), 122.03 (s, B(C$_6$H$_5$)$_4^-$), 125.87 (m, J_{CB} = 2.9 Hz, B(C$_6$H$_5$)$_4^-$), 137.35 (m, J_{CB} = 1.4 Hz, B(C$_6$H$_5$)$_4^-$), 165.35 (q, J_{CB} = 49.5 Hz, B(C$_6$H$_5$)$_4^-$).

[Ru$_2$(μ-Cl)$_3${(^{i}Pr$_2$PCH$_2$CH$_2$)$_2$O}$_2$]BPh$_4$ is an orange powder that shows good and fair solubility in CH$_2$Cl$_2$ and tetrahydrofuran, respectively. It is insoluble in methanol, isooctane, and benzene.

Preparation of [Ru$_2$(μ-Cl)$_3${(^{i}Pr$_2$PCH$_2$CH$_2$)$_2$O}$_2$}][PF$_6$] (2·PF$_6$). A 6 mL methanol solution of LiPF$_6$ (71 mg, 0.47 mmol) was added dropwise to a stirred methanol (4 mL) solution of [Ru$_2$(μ-Cl)$_3${(^{i}Pr$_2$PCH$_2$CH$_2$)$_2$O}$_2$}]Cl (102 mg, 0.107 mmol). The solution was stirred for 30 min. The solution was place in a −28 °C freezer for 1−2 days. Red crystals were collected by decantation and washed with isooctane (2 × 3 mL). Yield: 73%. Anal. Calcd for C$_{32}$H$_{72}$Cl$_3$F$_6$O$_2$P$_5$Ru$_2$: C, 36.05; H, 6.81. Found: C, 35.81; H, 6.63. ^{1}H NMR (acetone-d_6): δ 1.32−1.86 (m, 51H), 1.92−2.29 (m, 9H), 3.12−4.02 (m, 12H). ^{31}P{^{1}H} NMR (acetone-d_6): δ −143.1 (septet, $^1J_{PF}$ = 5.8 Hz, PF$_6^-$), 64.4 (d, $^2J_{PP}$ = 29.6 Hz), 73.1 (d, $^2J_{PP}$ = 29.6 Hz). ^{13}C{^{1}H} NMR (acetone-d_6): δ 19.09 (d, $^2J_{CP}$ = 8.3 Hz, PC*C*H$_3$), 19.76 (d, $^2J_{CP}$ = 7.8 Hz, PC*C*H$_3$), 20.42 (d, $^2J_{CP}$ = 3.8 Hz, PC*C*H$_3$), 20.58 (d, $^2J_{CP}$ = 5.8 Hz, PC*C*H$_3$), 20.85 (d, $^2J_{CP}$ = 3.2 Hz, PC*C*H$_3$), 20.94 (d, $^2J_{CP}$ = 1.5 Hz, PC*C*H$_3$), 21.15 (s, PC*C*H$_3$), 21.39 (d, $^2J_{CP}$ = 2.6 Hz, PC*C*H$_3$), 25.99 (d, $^1J_{CP}$ = 24.1 Hz, P*C*H$_2$), 27.95 (d, $^1J_{CP}$ = 23.9 Hz, P*C*H), 29.81 (d, $^1J_{CP}$ = 25.0 Hz, P*C*H$_2$), 29.81 (d, $^1J_{CP}$ = 21.0 Hz, P*C*H), 30.48 (d, $^1J_{CP}$ = 19.0 Hz, P*C*H), 32.49 (d, $^1J_{CP}$ = 23.1 Hz, P*C*H), 77.22 (s, O*C*H$_2$), 79.00 (s, OCH$_2$).

[Ru$_2$(μ-Cl)$_3${(^{i}Pr$_2$PCH$_2$CH$_2$)$_2$O}$_2$}]PF$_6$ is a red crystalline material that has good solubility in tetrahydrofuran and acetone but only fair solubility in methanol. It is insoluble in isooctane and benzene.

Preparation of Ru(H$_2$)Cl$_2${(^{t}Bu$_2$PCH$_2$CH$_2$)$_2$O} (3). A suspension of **1** (103 mg, 0.193 mmol) in 4 mL of benzene was degassed and placed under an atmosphere of H$_2$ (∼3 psi). The suspension was heated to 50 °C for 2 h, then allowed to cool to ambient temperature for 1 h. The solid product was collected by filtration, washed with hexane (2 × 3 mL), and dried in vacuo. Yield: 86 mg (83%). Anal. Calcd for C$_{20}$H$_{46}$Cl$_2$OP$_2$Ru: C, 44.78; H, 8.64. Found: C, 44.99; H, 8.39. ^{1}H NMR (C$_6$D$_6$): δ −10.1 (t, $^2J_{HP}$ = 8.8 Hz, 2H, Ru(*H*$_2$)), 1.01 (m, 2H, PC*H*$_2$), 1.21 (vt, ^vJ = 12.3 Hz, 18H, PC(C*H*$_3$)$_3$), 1.60 (m, 2H, PC*H*$_2$), 1.68 (vt, ^vJ = 12.9 Hz, 18H, PC(C*H*$_3$)$_3$), 2.59 (m, 2H, OC*H*$_2$), 3.52 (m, 2H, OC*H*$_2$). ^{31}P{^{1}H} NMR (C$_6$D$_6$, 298 K): δ 61.4 (s). ^{13}C{^{1}H} NMR (C$_6$D$_6$): δ 24.4 (vt, ^vJ = 10.6 Hz, P*C*H$_2$), 25.5 (s, P*C*H$_2$), 30.6 (vt, ^vJ = 4.6 Hz, PC(*C*H$_3$)$_3$), 31.6 (vt, ^vJ = 4.3 Hz, PC(*C*H$_3$)$_3$), 35.0 (vt, ^vJ = 15.5 Hz, P*C*(CH$_3$)$_3$), 39.7(vt, ^vJ = 9.5 Hz, P*C*(CH$_3$)$_3$), 75,32 (s, O*C*H$_2$).

Ru(η^2-H$_2$)Cl$_2${(^{t}Bu$_2$PCH$_2$CH$_2$)$_2$O} is an orange powder that is sparingly soluble in tetrahydrofuran, benzene, or toluene. It is insoluble in hexane and like solvents.

Preparation of Ru(HD)Cl$_2${(^{t}Bu$_2$PCH$_2$CH$_2$)$_2$O} (3-*d*). A C$_6$D$_6$ (0.65 mL) solution of **3** (15 mg) was placed in a Wilmad NMR tube with a J-Young valve. The solution was subjected to three freeze−pump−thaw cycles and backfilled with gaseous D$_2$. The solution was vigorously shaken for 15 min, then heated to 50 °C for a few minutes. The ^{1}H NMR spectrum showed a mixture of **3** and Ru(HD)Cl$_2${(^{t}Bu$_2$PCH$_2$CH$_2$)$_2$O} in a ratio of 2:3, respectively. Allowing the solution to stand overnight at ambient temperature resulted in near complete transformation to Ru(D$_2$)Cl$_2${(^{t}Bu$_2$PCH$_2$CH$_2$)$_2$O}.

Preparation of [Ru(N$_2$)Cl{(^{t}Bu$_2$PCH$_2$CH$_2$)$_2$O}][BPh$_4$]·CH$_2$Cl$_2$ (4). Dichloromethane (3 mL) was added to a mixture of RuCl$_2${(^{t}Bu$_2$PCH$_2$CH$_2$)$_2$O} (104 mg, 0.195 mmol) and NaBPh$_4$ (67 mg, 0.196). The mixture was vigorously stirred for 3 h. After crystallization of NaCl (−30 °C, overnight) the mixture was filtered. The volume of the filtrate was reduced to approximately 1 mL, and hexane (0.5 mL) was added. The solution was placed in a −30 °C freezer overnight. A dark crystalline material was collected by filtration and washed with hexane (3 × 1.5 mL). Yield: 148 mg (90%). Anal. Calcd for C$_{45}$H$_{66}$BCl$_3$N$_2$OP$_2$Ru: C, 58.04; H, 7.14; N, 3.01. Found: C, 58.31; H, 7.37; N, 2.99. IR: ν(N≡N) 2143 cm^{-1} (KBr and Nujol). ^{1}H NMR (CD$_2$Cl$_2$, 297 K): δ 0.48, 1.48 (br s, PC(C*H*$_3$)$_3$), 1.90 (m, 2H, PC*H*$_2$), 2.00 (m, 2H, PC*H*$_2$), 3.71 (m, 2H, OC*H*), 3.91 (m, 2H, OC*H*), 6.96, 7.16, 7.58 (m, 20H, B*Ph*$_4^-$). ^{31}P{^{1}H} NMR (CD$_2$Cl$_2$, 297 K): δ 54.6 (s). ^{1}H NMR (CD$_2$Cl$_2$, 273 K): δ 0.44 (vt, ^vJ = 6.5 Hz,18H, PC(C*H*$_3$)$_3$), 1.46 (vt, ^vJ = 7.4 Hz, 18H, PC(C*H*$_3$)$_3$), 1.84 (m, 2H, PC*H*$_2$), 2.01 (m, 2H, PC*H*$_2$), 3.63 (m, 2H, OC*H*), 3.86 (m, 2H, OC*H*), 6.96, 7.16, 7.58 (m, 20H, B*Ph*$_4^-$). ^{31}P{^{1}H} NMR (CD$_2$Cl$_2$, 273 K): δ 53.8 (s). ^{1}H NMR (CD$_2$Cl$_2$, 173 K): δ −2.05 (br s, 6H, PC(C*H*$_3$)), 1.13, 1.36, 1.54 (br s, 34H, PC(C*H*$_3$)$_3$, PCH$_2$), 3.31 (br, 2H, OC*H*$_2$), 3.59 (br, 2H, OC*H*$_2$), 6.82, 7.01, 7.39 (m, 20H, B*Ph*$_4^-$). ^{31}P{^{1}H} NMR (CD$_2$Cl$_2$, 173 K): δ 51.0 (s).

[RuCl(N$_2$){(^{t}Bu$_2$PCH$_2$CH$_2$)$_2$O}][BPh$_4$] is an air-sensitive dark colored crystalline material that is soluble in CH$_2$Cl$_2$ and tetrahydrofuran and insoluble in hexane.

Preparation of Ru(H$_2$)Cl$_2${(^{i}Pr$_2$PCH$_2$CH$_2$)$_2$O} (5). A 2-methyl-2-butanol (10 mL) solution of [RuCl$_2$(*p*-cymene)]$_2$ (329 mg, 0.537 mmol) and (^{i}Pr$_2$PCH$_2$CH$_2$)$_2$O (342 mg, 1.12 mmol) was degassed and placed under an atmosphere of H$_2$ (∼3 psi). The mixture was heated to 90 °C for 26 h. Deep red crystals

formed after cooling to ambient temperature overnight (~16 h). The crystals were collected by filtration and washed with isooctane (3 × 3 mL). Recrystallization of the supernatant afforded a second crop of product. Yield: 308 mg (60%). Anal. Calcd for $C_{16}H_{38}Cl_2OP_2Ru$: C, 40.00; H, 7.97. Found: C, 40.22; H, 7.84. ^{1}H NMR (C_6D_6): δ −14.7 (s, 2H, Ru(H_2)), 1.23 (d vt, $^3J_{HH}$ = 6.7 Hz, ^vJ = 13.4 Hz, 12H, PC(CH_3)$_2$), 1.42 (d vt, $^3J_{HH}$ = 7.8 Hz, ^vJ = 15.5 Hz, 12H, PC(CH_3)$_2$), 1.86 (m, 4H, PCH_2), 3.00 (m, 4H, PCH), 3.51 (m, 4H, OCH_2). ^{31}P{^{1}H} NMR (C_6D_6): δ 64.7 (s). ^{13}C{^{1}H} NMR (C_6D_6): δ 19.2 (s, PC(*C*H$_3$)$_2$), 20.9 (vt, ^vJ = 1.8 Hz, PC(*C*H$_3$)$_2$), 21.97 (vt, ^vJ = 11.5 Hz, P*C*H), 26.48 (vt, ^vJ = 7.5 Hz, P*C*H$_2$), 73.5 (vt, ^vJ = 2.4 Hz, O*C*H$_2$).

Ru(H_2)Cl_2{(^{i}Pr$_2$PCH$_2$CH$_2$)$_2$O} is a red crystalline material that is soluble in benzene, toluene, and to a lesser extent 2-methyl-2-butanol. It has poor solubility in isooctane. It is air stable for several days in solid form.

Preparation of Ru(HD)Cl$_2${(^{i}Pr$_2$PCH$_2$CH$_2$)$_2$O} (5-*d*). A C_6D_6 (0.65 mL) solution of **5** (11 mg) was placed in a Wilmad NMR tube with a J-Young valve. The solution was subjected to three freeze−pump−thaw cycles and backfilled with gaseous D_2. The solution was heated to 50 °C for a few minutes, then vigorously shaken for 15 min. The ^{1}H NMR spectrum showed a mixture of **5** and Ru(HD)Cl_2{(^{i}Pr$_2$PCH$_2$CH$_2$)$_2$O} in a ratio of 3:7, respectively. Allowing the solution to stand overnight at ambient temperature resulted in near complete transformation to Ru(D_2)Cl_2{(^{i}Pr$_2$PCH$_2$CH$_2$)$_2$O}.

Preparation of RuCl$_2$(N$_2$){(^{i}Pr$_2$PCH$_2$CH$_2$)$_2$O} (6). A stirred 2-methyl-2-butanol (12 mL) solution of [Ru$_2$(μ-Cl)$_3${(^{i}Pr$_2$PCH$_2$CH$_2$)$_2$O}$_2$]Cl (206 mg, 0.215 mmol) was heated to 75 °C for 2 h under a N_2 atmosphere. The solvent was removed in vacuo, and the products crystallized from a toluene/isooctane mixture at −28 °C. Yield: 180 mg (83%). Anal. Calcd for $C_{16}H_{36}Cl_2N_2OP_2Ru$: C, 37.95; H, 7.17. Found: C, 38.20; H, 7.12. IR: ν(N≡N) 2119.0 cm^{-1} (Nujol), 2114.6 cm^{-1} (KBr). ^{1}H NMR (C_6D_6): δ 1.23 (d vt, $^3J_{HH}$ = 7.2 Hz, ^vJ = 13.3 Hz, 12H, PC(CH_3)$_2$), 1.43 (d vt, $^3J_{HH}$ = 7.5 Hz, ^vJ = 15.3 Hz, 12H, PC(CH_3)$_2$), 1.62 (m, 4H, PCH_2), 3.08 (m, 4H, PCH), 3.26 (m, 4H, OCH_2). ^{31}P{^{1}H} NMR (C_6D_6): δ 48.3 (s). ^{13}C{^{1}H} NMR (C_6D_6): δ 19.04 (s, PC(*C*H$_3$)$_2$), 20.45 (vt, ^vJ = 2.9 Hz, PC(*C*H$_3$)$_2$), 22.91 (vt, ^vJ = 21.6 Hz, P*C*H), 25.75 (vt, ^vJ = 16.1 Hz, P*C*H$_2$), 74.00 (vt, ^vJ = 4.3 Hz, O*C*H$_2$).

RuCl$_2$(N$_2$){(^{i}Pr$_2$PCH$_2$CH$_2$)$_2$O} is a yellow crystalline material that shows good soluble in benzene, toluene, and CH_2Cl_2 but only fair solubility in 2-methyl-2-butanol. The compound shows poor solubility in hexane and isooctane. The compound is air stable in solid form for several days.

X-ray Crystallographic Analyses. For all compounds, data were collected on a Nonius Kappa-CCD diffractometer using monochromated Mo Kα (wavelength = 0.71073 Å) radiation. Each data set was measured using a combination of ϕ scans and ω scans with κ offsets, to fill the Ewald sphere. The data were processed using the Denzo-SMN package.[21] Absorption corrections were carried out using SORTAV.[22] The structures were solved and refined using SHELXTL V6.1[23] for full-matrix least-squares refinements that were based on F^2. The H atoms were placed in calculated positions and included in the structure refinement in a riding motion approximation. The hydride atoms in **6** were refined independently, and their thermal parameters were tied to that of the Ru atom such that U_{iso}(H) = 1.5U_{eq}(Ru). Crystallographic data for complexes **1**, **2**·PF_6, **4**, **5**, and **6** are provided in CIF format with the Supporting Information.

Computational Details. The calculations were done with Gaussian 03 (Revision B05) and GaussView (version 3.09) programs.[24] All geometries were fully optimized without symmetry or internal coordinate constraints using the *m*PW1PW91 functional, which included modified Perdew−Wang exchange and Perdew−Wang 91 correlation.[25] The nature of the stationary points **3′**, **3″**, **5′**, **5″**, **3′ts**, and **5″ts** was verified by frequency calculations, which were used to calculate ZPE without scaling. The basis set employed in the calculations included SDD + ECP for Ru, 6-31G(p) for the coordinated H_2, 6-31G for all CH_3 groups, and 6-31G(d) for the rest of the atoms.[26]

Acknowledgment. We gratefully acknowledge the Natural Sciences and Engineering Research Council of Canada (NSERC) and the Ontario Government for funding.

Supporting Information Available: Atomic coordinates of the calculated complexes and crystallographic data for complexes **1**, **2**·PF_6, **4**, **5**, and **6**. This material is available free of charge via the Internet at http://pubs.acs.org.

OM050053V

(21) Otwinowski, Z.; Minor, W. In *Methods in Enzymology*: *Macromolecular Crystallography*; Carter, C. W., Sweet, R. M., Eds.; Academic Press: London, 1997; Vol. 276, part A, pp 307−326.

(22) Blessing, R. H. *Acta Crystallogr.* **1995**, *A51*, 33.

(23) Sheldrick, G. M. *SHELXTL/PC*, Version 6.1 Windows NT Version; Bruker AXS Inc.: Madison, WI, 2001.

(24) Frisch, M. J.; Trucks, G. W.; Schlegel, H. B.; Scuseria, G. E.; Robb, M. A.; Cheeseman, J. R.; Zakrzewski, V. G.; Montgomery, J. A., Jr.; Stratmann, R. E.; Burant, J. C.; Dapprich, S.; Millam, J. M.; Daniels, A. D.; Kudin, K. N.; Strain, M. C.; Farkas, O.; Tomasi, J.; Barone, V.; Cossi, M.; Cammi, R.; Mennucci, B.; Pomelli, C.; Adamo, C.; Clifford, S.; Ochterski, J.; Petersson, G. A.; Ayala, P. Y.; Cui, Q.; Morokuma, K.; Salvador, P.; Dannenberg, J. J.; Malick, D. K.; Rabuck, A. D.; Raghavachari, K.; Foresman, J. B.; Cioslowski, J.; Ortiz, J. V.; Baboul, A. G.; Stefanov, B. B.; Liu, G.; Liashenko, A.; Piskorz, P.; Komaromi, I.; Gomperts, R.; Martin, R. L.; Fox, D. J.; Keith, T.; Al-Laham, M. A.; Peng, C. Y.; Nanayakkara, A.; Challacombe, M.; Gill, P. M. W.; Johnson, B.; Chen, W.; Wong, M. W.; Andres, J. L.; Gonzalez, C.; Head-Gordon, M. E.; Replogle, S.; Pople, J. A. *Gaussian 03* (Revision B05) and *GaussView* (version 3.09); Gaussian, Inc.: Pittsburgh, PA, 2001.

(25) (a) Adamo, C.; Barone V. *J. Chem. Phys.* **1998**, *108*, 664. (b) Perdew, J. P.; Burke, K.; Wang, Y., *Phys. Rev. B* **1996**, *54*, 16533. (c) Burke K.; Perdew, J. P.; Wang, Y. In *Electronic Density Functional Theory: Recent Progress and New Directions*; Dobson, J. F., Vignale, G., Das, M. P., Eds.; Plenum: New York, 1998.

(26) For more information about the basis sets implemented in Gaussian 03 and detailed references see: Frish, A.; Frish, M. J.; Trucks, G. W. *Gaussian 03 User's Reference*; Gaussian, Inc.: Pittsburgh, PA, 2003. The basis sets are also available from the Extensible Computational Chemistry Environment Basis Set Database (www.emsl.pnl.gov/forms/basisform.html), which is developed and distributed by the Molecular Science Computing Facility, Environmental and Molecular Sciences Laboratory, which is part of the Pacific Northwest Laboratory, P.O. Box 999, Richland, WA 99352.